Ecotoxicology and Environmental Safety 286 (2024) 117174

Contents lists available at ScienceDirect

Ecotoxicology and Environmental Safety

journal homepage: www.elsevier.com/locate/ecoenv

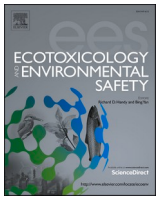

Danio rerio embryo as *in vivo* model for the evaluation of the toxicity and metabolism of pyrovalerone cathinones

P. García-Atienza [a], E. Sancho [b,*], M.D. Ferrando [b], S. Armenta [a,*]

[a] Analytical Chemistry Department, Universitat de València, 50th Dr. Moliner St, Burjassot 46100, Spain
[b] Cellular Biology, Functional Biology and Physical Anthropology Department, Universitat de València, 50th Dr. Moliner St, Burjassot 46100, Spain

ARTICLE INFO

Edited by Dr. Caterina Faggio

Keywords:
New psychoactive substances
Fish embryo toxicity test (FET)
Danio rerio embryo
Pyrovalerone cathinone metabolism

ABSTRACT

The objective of the present manuscript was the evaluation of the toxicity and metabolism of the second generation of pyrovalerone cathinones (α-PHP, α-PHPiP, 4-MePPP and TH-PVP), using an early zebrafish (*Danio rerio*) larvae as in vivo model. Pyrovalerone cathinones LC_{50} were determined after 24, 48, 72 and 96 h of exposure. TH-PVP proved to be the most toxic cathinone, whereas 4-MePPP was the least toxic. During acute exposure to pyrovalerone cathinones the main signs of toxicity exhibited by survivors were pericardial edema, yolk sac in embryos, bradycardia, delay in the hatching, malformations, and larvae without touch response. Afterwards, a short-term non-lethal experiment (24 h) was performed with early zebrafish larvae (72 h) for each of the selected compounds. The produced metabolites were tentatively identified by liquid chromatography-high resolution mass spectrometry (LC-HRMS) and the metabolic pathways were proposed. The results showed that hydroxylation and dihydroxylation can be considered the main metabolic pathways, although depending of the cathinone studied, other metabolites can be found.

1. Introduction

Synthetic cathinones are the second largest group of substances included in the new psychoactive substances (NPS) and have become the most seized class of NPS reported to the UNODC Early Warning Advisory system (La Maida et al., 2021). Different health problems have been associated with the use of synthetic cathinones, including cardiovascular disorders, hallucinations, and violent behavior (Coppola and Mondola, 2012; Soares et al., 2021), being identified in fatal intoxications, alone or in combination with other substances (La Maida et al., 2021). Pyrovalerone cathinones are a special sub-class of synthetic cathinones from the pharmacological effects point of view, because they mimic the psychostimulant effects of amphetamines and behave as pure blockers of monoamine uptake transporters (Rickli et al., 2015). 3,4-methylenedioxypyrovalerone (MDPV) has been the most representative compound of the family until it was considered as a controlled substance by international organizations (Kolanos et al., 2013). After that, a second generation of pyrovalerone derivatives irrupted into black markets (Soares et al., 2021), including 4-methyl-α-pyrrolidinopropiophenone (4-MePPP), 2-pyrrolidin-1-yl-1-(5,6,7,8-tetrahydronaphthalen-2-yl) pentan-1-one (TH-PVP), α-pyrrolidinohexanophenone (α-PHP), and α-pyrrolidinoisohexanophenone (α-PHiP) (Kolaczynska et al., 2021). α-PHP was first identified in 2014 (Uchiyama et al., 2014) and it has been recently, between 2017 and 2020, involved in several fatal intoxications reports (La Maida et al., 2021), while, α-PHiP was first reported to the European Monitoring Centre on Drugs and Drugs Addiction (EMCDDA) by Slovenia in 2016 (National Forensic Laboratory, 2016) and it has been also associated with fatal drug abuse cases (Adamowicz et al., 2020). In 2022, α-PHP and α-PHiP were included in the top five of synthetic cathinones by number of seizures and by quantity of material seized reported to the EU Early Warning System of the European Union (EMCDDA, 2024). 4-MePPP was identified in the late 1990s as a recreational stimulant in the German market. Later on, it was included in a controlled substance list by the German authorities, but has re-emerged on the black market in products that include a mixture of cathinones (Kolanos et al., 2013). In 2016, 4-MePPP was included in the schedule I of the Controlled Substances Act (Drug Enforcement Administration & Department of Justice, 2016). TH-PVP was identified in 2018 by the authorities as a substance of special concern (Drug Enforcement Administration and Department of Justice, 2018) due to its pharmacological effects and potential toxicity. Recent literature has demonstrated that the concentration of synthetic cathinones in wastewater has

* Corresponding authors.
E-mail addresses: encarna.sancho@uv.es (E. Sancho), sergio.armenta@uv.es (S. Armenta).

https://doi.org/10.1016/j.ecoenv.2024.117174
Received 30 July 2024; Received in revised form 1 October 2024; Accepted 9 October 2024
Available online 17 October 2024

increased in recent years (González-Mariño et al., 2016). α-pyrrolidinovalerophenone (α-PVP), 4-methyl-α-pyrrolidinohexiophenone (4-MePHP), and MDPV have been identified in wastewater samples of Adelaide (Tscharke et al., 2016), Milan, or Santiago de Compostela (González-Mariño et al., 2016). The incomplete degradation of those compounds in wastewater treatment plants makes that synthetic cathinones arrive to various environmental media (Castiglioni et al., 2021; Yao et al., 2021). Regrettably, psychoactive substance bioaccumulation and undesired biological activity have been previously reported in fish species such as zebrafish (*Danio rerio*) (De Felice et al., 2020; Souders et al., 2019) and there are evidences of bioaccumulation of α-PHP and α-PHiP in liver, kidney, brain, stomach, intestine, and heart (Adamowicz et al., 2020; Vignali et al., 2019). Thus, considering their unique pharmacological profiles and the public health concerns associated with these compounds, there is a need for further toxicological and potential ecological risk assessment studies.

Nowadays, there are three categories of toxicity models; *in silico*, performed via computer simulation, *in vivo*, which use living organisms as models, and *in vitro* models, which use an organ, tissue, or cell of a specific organism (Summerfield and Dong, 2013). The *in vivo* toxicity model stands out because it involves a whole organism, and it is often considered the most accurate for assessing drug toxicity. However, the most important drawback relies on the biological differences between humans and the animal species used in those models.

Danio rerio, also known as zebrafish, was proposed as *in vivo* model for toxicity studies by Streisinger et al. (1981) due to the similarities of their neurological pathways with mammals. The main advantages of zebrafish as *in vivo* model include that it is an intact, easy-to-handle and low-cost organism, the analysis of transparent embryos allows for noninvasive imaging techniques, and zebrafish embryos develop much faster than those of mammals, shortening experimentation time (Garcia et al., 2016). Moreover, the European Union considers that fish embryos are unprotected life stages until they acquire the ability of independent feeding (European Parliament & The Council Of The European Union, 2010). The period of independent feeding has been defined based on several criteria such as maturity of the digestive tract, and swimming ability, being set the limit at 120 h post fecundation (hpf) to be considered as non-protected life stages. Zebrafish larvae acquire metabolic detoxifying pathways after 72 hpf being those processes similar to those reported in mammals (Matos et al., 2020). Zebrafish are able to perform phase I and phase II metabolism reactions, and, thus, this model has been previously used to evaluate the toxicity and metabolism of synthetic cannabinoids (Morales-Noé et al., 2022), synthetic cathinones (Kolesnikova et al., 2019; Prado et al., 2021), hallucinogens (Wagmann et al., 2020) and emerging contaminants (De Oliveira Eiras et al., 2022). Phase I enzymes consist primarily of the cytochrome P450 (CYP) superfamily of microsomal enzymes, being CYP families 1–3 the enzymes involved in xenobiotic metabolism (Saad et al., 2016). It has been reported that many human CYP enzymes have direct orthologs in zebrafish (Goldstone et al., 2010), suggesting that zebrafish metabolic profiles may be similar to those of mammals.

In summary, this manuscript aimed to evaluate the zebrafish embryo acute toxicity of the selected drugs through the determination of the lethal concentration causing 50 % death (LC_{50}), study the metabolism of these compounds using an early zebrafish larvae as in vivo model, and compare the obtained data with those of previously reported in "classical" drugs to establish the potential toxicological behavior and ecological risk associated to pyrovalerone cathinones.

2. Material and methods

2.1. Standards and reagents

α-PHP, α-PHiP, 4-MePPP and TH-PVP standards were provided by Cayman Chemicals (Ann Arbor, MI, USA). A concentrated solution of 120 mg L^{-1} of each individual cathinone was prepared in dechlorinated tap water medium in amber glass vials. From these concentrated solutions, diluted solutions of each compound (α-PHP, α-PHiP, 4-MePPP and TH-PVP) were prepared for the acute toxicity test.

Methanol and buffer constituents were acquired from Scharlab (Barcelona, Spain).

2.2. Zebrafish (Danio rerio) embryos

Zebrafish eggs (wild-type, AB strain, adult zebrafish) were obtained from Aprende con Danio (Alicante, Spain). Danieau's medium were prepared according to previous references (Morales-Noé et al., 2022) and was used to transfer the fertilized eggs to the Ecotoxicology Laboratory (*Universitat de València*, Spain).

The fertilized eggs were washed three times with dechlorinated tap water and were placed in 15 mL Petri dishes with water. Zebrafish eggs were maintained in a climate-controlled chamber (16 h light and 8 h dark, 64 ft-c light intensity, and 26 ± 0.5 °C). Tap water was aerated to oxygen saturation before acclimatization and the start of the experiments. The total hardness of tap water was 180 ± 10 mg L^{-1} as $CaCO_3$, a pH value of 7.9 ± 0.2 and an alkalinity of 4.0 ± 0.5 mmol L^{-1}.

No mortality of zebrafish eggs was observed during the acclimatization period (24 h). A MZ125 stereo microscope from Leica Mikrosysteme Vertrieb GmbH (Wetzlar, Germany) was used to examine fertilized eggs and zebrafish embryos.

2.3. Acute toxicity test

The Organization for Economic Cooperation and Development (OECD) standard procedure 236 "Fish embryo acute toxicity (FET) test" (OECD, 2013) slightly adjusted to our laboratory conditions was employed in this study.

At the beginning of the experiments, embryos were at the developmental stage of 18–20 hpf at a temperature of 26 ± 0.5 °C (Kimmel et al., 1995). All embryos exhibited spontaneous tail contractions as an initial assessment of locomotion for the hatching process (Weichert et al., 2017).

A minimum number of five concentrations (up to 8 concentration levels), from 1 to 100 mg L^{-1} concentration range, of the cathinones, and a blank control (with water) were prepared and tested in the acute toxicity tests. The standard solutions of the cathinones were prepared the day before starting the experiments in graduated flasks by direct dilution of the standard in ultrapure water (18 MΩ cm^{-1}) without the addition of organic solvent. The Costar® multiple well plates (Corning, NY, USA) were conditioned with the solutions 24 h prior to the start of an experiment and kept in the incubator of the acclimatized chamber. During the testing period, pH and oxygen levels were in the range of the criteria of the OECD 236. Each assay was performed in a 24-well plate with 1 embryo (stage <20 hpf) per well with a final volume of 2 mL and six replicates per assay were performed. Assay plates were covered with self-adhesive film and kept in the benchtop incubator inside the climate-controlled chamber. The number of dead embryos were recorded every 24 h during the assays, being the apical endpoints coagulated embryos, no tail detachment and no heartbeat. Endpoints were recorded by direct observation of the zebrafish embryos with a MZ125 stereo microscope from Leica Mikrosysteme Vertrieb GmbH.

Additionally, the following non-lethal endpoints were also recorded: i) hatching rates, pericardial edema and/or yolk sac, bradycardia, spinal deformity, clotted tail, normal pigmentation level, melanophore pattern, response to touch, length compared to control group, swimming and resting position, as well as any evident observational effect different from the control groups. At the end of the experiments, the surviving embryos were euthanized.

2.4. Metabolism study

To study the metabolism of the four pyrovalerone cathinones in

zebrafish larvae, a short-term (24 h) exposure was conducted using non-lethal cathinone concentrations, corresponding to their non-lethal threshold ($LC_{0.01}$) at 96 hpf. The $LC_{0.01}$ corresponded to the estimated concentration of analytes causing death to 0.01 % tested embryos, being these concentrations 3.0 mg L^{-1} of TH-PVP, 9.0 mg L^{-1} of α-PHiP, 15.7 mg L^{-1} of α-PHP and 55.9 mg L^{-1} of 4-MePPP, respectively.

Prior to non-lethal experiments, fertilized eggs were allowed to develop in tap water for 72 hpf in a benchtop incubator (26 ± 0.5 °C) in the acclimatized chamber under the same conditions as described above. After this time, all larvae were at stage 80.35 hpf at 28.5 °C (Kimmel et al., 1995). Prior to the exposure experiments, all unhatched embryos were dechorionated.

Zebrafish larvae (n= 10), were placed in two Petri dishes (n= 5) and exposed to a final volume of 5 mL of the selected drug concentration diluted in dechlorinated tap water as exposure medium. Control animals were maintained under the same conditions in drug-free medium. Both control and exposed groups of early larvae remained alive for the stipulated exposure period. After 24 h of exposure, both water and early larvae were collected separately, recorded and stored frozen until metabolites determination.

2.5. LC-HRMS/MS instrumentation and conditions

The procedure described in (Morales-Noé et al., 2022) was used to evaluate the metabolism of the studied synthetic cathinones. Exposure medium was injected in the liquid chromatography-high resolution mass spectrometry (LC-HRMS/MS) after filtration through a 0.22 μm syringe filter. Larvae were lyophilized in a CRYODOS freeze dryer from Telstar Technologies S.L. (Terrassa, Spain) and extracted using 100 μL methanol. After 30 min manual agitation, the extracts were centrifuged for 2 min at 15,000 rpm, and transferred to autosampler vials for analysis.

The control samples, prepared in duplicate, used in this study imply the incubation of α-PHP, αPHiP, 4-MePPP and TH-PVP in a medium without the presence of zebrafish larvae to evaluate the possible degradation products of these compounds and the incubation of zebrafish larvae in a medium without pyrovalerone cathinones to assess the absence of interfering compounds.

Details of the analytical procedure can be found in (Morales-Noé et al., 2022). MS/MS spectral data were acquired using information-dependent acquisition (IDA) mode, being the accumulation time for the MS^1 full scan and IDA experiments, 100 and 50 ms, respectively. The criteria for selecting IDA data implied the MS/MS analysis of the most intense *m/z* signals (>1000 cps), dynamic background subtraction, 4 Da for the isotope exclusion window, and a half peak width of 2 s. Ion release delay and ion release width were set at 11 and 10 ms. The collision energy for the MS/MS experiments was set at 35 eV and *m/z* were scanned from 100 to 700 (*m/z*) with charge state +1. Data was evaluated using the PeakView™ software from AB SCIEX.

2.6. Statistical analysis

Mortality data were used to calculate 24, 48, 72 and 96 h LC_{50} values and their confidence limits (95 %) by Probit Regression Analysis, Chi test (χ^2) tested the goodness of the curve fit and its statistical significance. Any non-lethal effects observed during exposures were also used for calculations of their effective concentration 50, if possible. Calculations were performed using the Statistical Analysis System (SPSS, Chicago, IL, USA) with a significance level of 0.05.

3. Results and discussion

3.1. Acute toxicity test

No mortality was observed among control groups during the different experiments. At the end of the experimental time (96 h) the early larvae were measured. The standard length as distance from head to end of the tail, of the hatched embryos, was 3.96 ± 0.01 mm, this length corresponded to an early larvae stage < 120 hpf (28.5 °C) (Kimmel et al., 1995).

The 50 % lethal concentrations (LC_{50}) and their confidence limits were determined after 24, 48, 72 and 96 h of exposure (Table 1). TH-PVP proved to be the most toxic cathinone, whereas 4-MePPP proved to be the less toxic one. TH-PVP induced the greatest increase in toxicity in the range 24–96 h exposure (> 56 %) followed by α-PHiP (30 %) whereas 4-MePPP and α-PHP induced a 28.6 and 19.8 %, respectively.

The maximum concentration of cathinone at which all embryos survived and the minimum concentration causing 100 % mortality after 96 h were 1.88 and 6.50 mg L^{-1} (for TH-PVP); 16 and 18 mg L^{-1} (for α-PHP), 40 and 50 mg L^{-1} (for 4-MePPP); and 10 and 20 mg L^{-1} (for α-PHiP), respectively. During acute exposure to the different substances, the surviving embryos showed a series of toxic symptoms, including: pericardial edema and/or yolk sac -unhatched embryos-associated with bradycardia and early hatching <72 h (exposed to TH-PVP); non-hatched embryos and spinal malformation in early larvae (α-PHP), non-hatched embryos and no touch response in early larvae (4-MePPP); and non-hatched embryos plus severe bradycardia and no touch response in early larvae (α-PHiP) (See Fig. SM1). It has been previously demonstrated that cardiovascular physiology is conserved between humans and zebrafish at anatomical, cellular, and membrane-biology levels (Cassar et al., 2020) and, thus, zebrafish have been shown to provide a good model for cardiotoxicity. Many human cardiovascular drugs have shown comparable effects on zebrafish physiology (Macrae and Fishman, 2002). The touch-evoked response test is used as an indicator of neurotoxic effects. This test tracks the behavior of zebrafish larvae in response to a tactile stimulus given to the head or tail (Colwill and Creton, 2011). Previous studies have suggested that exists a close relationship between the dopamine system and larval zebrafish behavior, and there may be a direct link between dopamine D1 receptor and locomotor activity (Souders et al., 2019).

Fig. 1 shows the concentration-mortality curves of the different cathinones at 96 h exposure, which showed different shapes depending on the selected compound. All the tested compounds showed a sigmoidal toxicity curve indicating the presence of a threshold dose that induced the embryos mortality. From the obtained results, it can be observed that TH-PVP is the most toxic evaluated substance, being a potentially dangerous compound with a narrow concentration range between no observable effects and 100 % of individuals dead, while the other three compounds exhibited a wider range. 4-MePPP showed the least pronounced form of the curve slope, as shown by the lowest toxic effect observed.

It has been previously reported that the α-carbon chain may contribute to adverse side effects of unsubstituted pyrrolidine cathinones (Chen and Canal, 2020). The increase of the chain length from one carbon (α-PPP) to four (α-PHP) causes an increase in dopamine transporters (DAT) affinity and dopamine reuptake inhibition potency (Eshleman et al., 2017). The differences in DAT potency, however, between α-PVP and α-PHP are not significant, yet α-PHP reportedly produces more pronounced tachycardia than α-PVP (Chen and Canal, 2020). In this sense, preclinical cytotoxicity studies using dopaminergic SH-SY5Y cells show that α-PPP and α-PBP are less potent than α-PVP, with LC_{50} values at millimolar concentrations that far exceed their half maximal inhibitory concentration (IC_{50}) potencies at DAT and NET (Soares et al., 2019), suggesting pharmacodynamic effects beyond DAT and NET. Moreover, an increase of the length of the α-carbon side chain of pyrovalerone cathinones caused a steep increase in affinity at all muscarinic receptor antagonists subtypes, while the presence of a methylenedioxy moiety generally hindered this effect (Soares et al., 2019).

In order to have a more specific view of the toxicity of the substances tested, the obtained LC_{50} values have been compared with other values previously published in the literature for better-known substances. In this sense, it has been reported LC_{50} values for 24 h acute zebrafish

Table 1
Calculated LC_{50} values and 95 % confidence limits between brackets (mg L^{-1}) in *Danio rerio* embryos for the different second generation pyrovalerone cathinones at different exposure times.

	Exposure time (h)			
Compound	**24**	**48**	**72**	**96**
α-PHP	27.82 (27.17–28.64)	24.45 (24.03–24.86)	23.96 (22.69–25.69)	22.30 (24.50–23.29)
α-PHiP	56.37 (53.49–59.36)	48.78 (34.85–54.73)	45.90 (31.24–53.39)	39.39 (35.86–43.59)
4-MePPP	93.32 (84.45–132.47)	76.53 (73.54–79.86)	68.21 (66.06–71.70)	65.62 (64.84–68.97)
TH-PVP	11.04 (10.49–11.69)	6.85 (5.62–6.34)	5.32 (5.06–5.62)	4.78 (4.53–5.04)

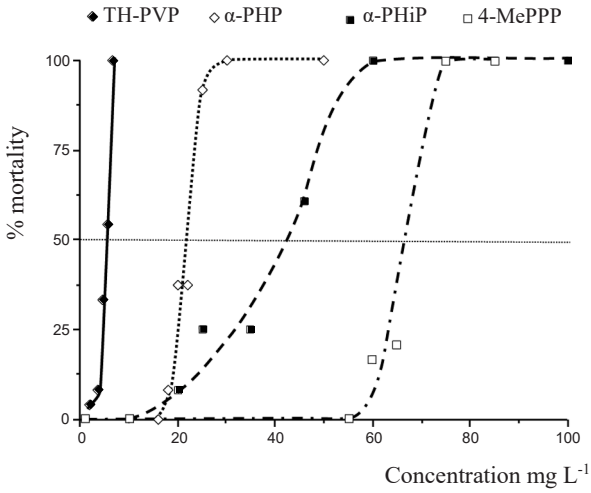

Fig. 1. Concentration-Mortality (%) curves of *Danio rerio* embryos exposed to the different evaluated compounds after 96 h of exposure in static conditions.

toxicity test for cocaine (143 mg L^{-1}), MDPV (37 mg L^{-1}), MDMA (35 mg L^{-1}), methylone (26 mg L^{-1}), and mephedrone(26 mg L^{-1}) (Teixidó et al., 2023). On the other hand, TH-PVP presented LC_{50} values lower than those of potent toxic compounds such as, morphine (9915 mg L^{-1}), nicotine (35 mg L^{-1}), atropine (607 mg L^{-1}), aconitine (34 mg L^{-1}), strychnine (21 mg L^{-1}), and amitriptyline (8 mg L^{-1}) (Ali et al., 2011).

3.2. Metabolism

As it has been commented, zebrafish embryos were exposed to the $LC_{0.01}$ of each substance to study the metabolism of the four different second generation pyrovalerone cathinones. After the experiment, it was found that all zebrafish larvae had survived, but some embryos exhibited different symptoms. Larvae exposed to TH-PVP steady laterally without touch-evoke response, while larvae exposed to α-PHiP and 4-MePPP exhibited bradycardia and no touch response. Those exposed to α-PHP exhibited tachycardia as well as strong heartbeat compared to the control group. It should be mentioned that all metabolites proposed in this section were not present in control samples.

Table 2 shows the analytical features regarding molecular mass and elemental composition, fragmentation pattern, and retention time of the parent compounds and the putative metabolites. As no direct comparison with reference standards has been performed, all the proposed metabolites and metabolic pathways should be considered as putative.

It has been previously reported that human CYP enzymes including CYP2B6, CYP2C19, CYP2D6, and CYP1A2 were found to be responsible for synthetic cathinone metabolism (Contrucci et al., 2020; Meyer et al., 2010) Studies on the metabolism of the α-pyrrolidinophenone designer drug methylenedioxy-pyrovalerone (MDPV) in rat and human urine and human liver microsomes using GC-MS and LC-high-resolution MS and its detectability in urine by GC-MS (Meyer et al., 2010). Hydroxylation of the propyl side chain of α-PVP was catalyzed by human CYP2B6, CYP2C19, CYP2D6, and CYP3A4 isoforms (Sauer et al., 2009). In this sense, pyrovalerone cathinones such as alpha-pyrrolidinobutyro phenone (α-PBP), alpha-pyrrolidinopentiothiophenone (α-PVT), α-PHP, alpha-pyrrolidinoenanthophenone (α-PEP, PV8) and alpha-pyrrolidinooctanophenone (α-POP, PV9) are catalyzed by CYP 1A2, CYP2B6, CYP2C9, CYP2C19, CYP2D6, and CYP3A4 resulting in pyrrolidine, thiophene, or alkyl hydroxy metabolites based on alkyl chain length (Manier et al., 2018). This study reported that the CYP enzymes increase the affinity with the increase of alkyl chain length. CYP2C19 and CYP2D6 are responsible for metabolizing α-PBP, while CYP1A2, CYP2C9, and CYP2C19 metabolized α-PVT, α-PHP, α-PEP, and α-POP.

In this sense, the metabolic function of zebrafish CYP has been identified and their phylogenetic and shared syntenic relationships to human CYPs has been examined in detail (Goldstone et al., 2010). For instance, a direct relationship has been established in human CYP1A1/1A2 and CYP3A3,4,7 activity with zebrafish CYP1A and CYP3C1–4 in xenobiotic metabolism processes. Moreover, the single zebrafish CYP1B1 gene has a structure very similar to human CYP1B1. It has been reported that similar than mammals, the CYP2 constitutes the largest CYP gene family in zebrafish. Genes CYP2Y CYP2Y3 and CYP2Y4 share synteny with a cluster of CYP2 genes for human drug-metabolizing enzymes, including CYP2A6, CYP2A13, CYP2B6, CYP2F1, and CYP2S1. In summary, those zebrafish CYP families are probably the enzymes involved in pyrovalerone cathinone metabolism.

3.2.1. 4-MePPP metabolism

The structures of the metabolites, postulated from the MS/MS data and interpreted in correlation to those previously published in the scientific literature, were depicted in Fig. SM2.

As it can be seen, 4-MePPP parent compound presented a peak with a retention time of 6.83 min and a 218.1530 *m/z* value. MS/MS fragmentation showed two intense peaks with *m/z* values of 147.0804 (loss of pyrrolidine moiety) and 119.0964 (4-methylphenone group itself).

The tentatively proposed metabolic pathway of 4-MePPP included hydroxylation of the pyrrolidine and/or alkyl chain moieties (M1-M4) with *m/z* values of 234.1491 at retention times of 4.27–7.53 min, with at least four peaks. The main fragments observed in these peaks corresponded to the loss of a water molecule (216.1591) and the 4-methylphenone group (119.0604), which discarded the presence of the hydroxyl group in the phenone moiety. It should be highlighted that this metabolite could be also assigned to a keto-oxidation in the pyrrolidine group and a reduction of the carboxylic group of the cathinone.

Pyrrolidinyl oxidation (+O –2H) with *m/z* 232.1330 has been also putative identified (M5). MS/MS fragments at 119.0965, corresponding to the 4-methylphenone group and that at 112.0861 revealed oxidation and dehydrogenation in the pyrrolidine ring. Moreover, late elution of this metabolite (10.56 min) compared to 4-MePPP agrees to the oxidation of the pyrrolidinyl moiety that prevents the formation of hydrogen bonds (Swortwood et al., 2016). This biotransformation has been

Table 2
Retention time, accurate mass, elemental composition, mass error, and observed fragmentation of the parent compounds evaluated and the tentatively identified metabolites.

Compound	Retention time (min)	$[M+H^+]$ (*m/z*)	Elemental composition	Mass error (ppm)	Product ion (*m/z*)	Elemental composition
4-MePPP	6.83	218.1542	$C_{14}H_{19}NO^+$	1.20	147.0804	$C_{10}H_{11}O^+$
					119.0964	$C_8H_7O^+$
M1-M3	4.27–6.73	234.1491	$C_{14}H_{19}NO_2^+$	1.00	216.1591	$C_{14}H_{17}NO^+$
					119.0604	$C_8H_7O^+$
M4	7.53	234.1495	$C_{14}H_{19}NO_2^+$	2.80	216.1591	$C_{14}H_{17}NO^+$
					119.0604	$C_8H_7O^+$
M5	10.56	232.1335	$C_{14}H_{17}NO_2^+$	1.30	214.1433	$C_{14}H_{15}NO^+$
					147.0942	$C_{10}H_{11}O^+$
					119.0965	$C_8H_7O^+$
					112.0861	$C_6H_{10}NO^+$
M6	4.60	250.1444	$C_{14}H_{19}NO_3^+$	2.50	232.1554	$C_{14}H_{17}NO_2^+$
					214.1430	$C_{14}H_{15}NO^+$
					196.1305	$C_{14}H_{13}N^+$
					147.0804	$C_{10}H_{11}O^+$
					119.0964	$C_8H_7O^+$
TH-PVP	10.30	286.2164	$C_{19}H_{27}NO^+$	0.90	215.1849	$C_{15}H_{19}O^+$
					159.1116	$C_{11}H_{11}O^+$
					145.1292	$C_{11}H_{13}^+$
					126.1520	$C_8H_{16}N^+$
M'1-M'5	8.08–8.83	302.2115	$C_{19}H_{27}NO_2^+$	0.10	213.1701	$C_{15}H_{17}O^+$
					175.1101	$C_{12}H_{15}O^+$
					143.1137	$C_{11}H_{11}^+$
					126.1525	$C_8H_{16}N^+$
M'6-M'8	9.90–10.57	302.2116	$C_{19}H_{27}NO_2^+$	0.50	284.2565	$C_{19}H_{25}NO^+$
					159.1116	$C_{11}H_{11}O^+$
					145.1292	$C_{11}H_{13}^+$
M'9	8.94	300.1964	$C_{19}H_{25}NO_2^+$	2.00	229.1676	$C_{15}H_{17}O_2^+$
					211.1529	$C_{15}H_{15}O^+$
					173.0936	$C_{11}H_9O_2^+$
					126.1522	$C_8H_{16}N^+$
M'10	10.13	318.2068	$C_{19}H_{27}NO_3^+$	1.40	300.2555	$C_{19}H_{25}NO_2^+$
					282.2413	$C_{19}H_{23}NO^+$
					264.2272	$C_{19}H_{21}N^+$
					159.1116	$C_{11}H_{11}O^+$
					145.1295	$C_{11}H_{13}^+$
M'11	9.88	232.1702	$C_{15}H_{21}NO^+$	2.60	214.2008	$C_{15}H_{19}N^+$
					172.1456	$C_{12}H_{14}N^+$
					159.1116	$C_{11}H_{11}O^+$
					145.1292	$C_{11}H_{13}^+$
α-PHP	13.46	246.1840	$C_{16}H_{23}NO^+$	4.40	189.1387	$C_{12}H_{15}NO^+$
					175.1117	$C_{12}H_{15}O^+$
					140.1432	$C_9H_{18}N^+$
					119.0491	$C_8H_7O^+$
					105.0332	$C_7H_5O^+$
M''1-M'2	13.37–13.48	262.1793	$C_{16}H_{23}NO_2^+$	2.00	244.1701	$C_{16}H_{21}NO^+$
					188.1075	$C_{12}H_{14}NO^+$
					140.1610	$C_9H_{18}N^+$
					107.0628	$C_7H_7O^+$
					105.0465	$C_7H_5O^+$
M''3	13.91	278.1740	$C_{16}H_{23}NO_3^+$	3.20	260.1641	$C_{16}H_{21}NO_2^+$
					242.1532	$C_{16}H_{19}NO^+$
					174.1512	$C_{12}H_{14}O^+$
					105.0332	$C_7H_5O^+$
M''4	13.39–13.87	260.1646	$C_{16}H_{21}NO_2^+$	1.50	242.1844	$C_{16}H_{19}NO^+$
					175.1349	$C_{12}H_{15}O^+$
					157.1207	$C_{12}H_{13}^+$
					105.0464	$C_7H_5O^+$
α-PHiP	8.10	246.1852	$C_{16}H_{23}NO^+$	0.80	188.1137	$C_{12}H_{14}NO^+$
					140.1418	$C_9H_{18}N^+$
					119.0482	$C_8H_7O^+$
					105.0323	$C_7H_5O^+$
M*2	8.84	262.1810	$C_{16}H_{23}NO_2^+$	0.23	157.1012	$C_9H_{19}NO^+$
					105.0330	$C_7H_5O^+$
M*3	7.50	262.1798	$C_{16}H_{23}NO_2^+$	0.20	244.1670	$C_{16}H_{21}NO^+$
					188.1067	$C_{12}H_{14}NO^+$
					156.1374	$C_9H_{18}NO^+$
					119.0488	$C_8H_7O^+$
					105.0323	$C_7H_5O^+$
M*4	6.83	262.1784	$C_{16}H_{23}NO_2^+$	0.23	205.1099	$C_{12}H_{14}NO_2^+$
					140.1431	$C_9H_{18}N^+$
					121.0486	$C_8H_9O^+$
					107.0485	$C_7H_7O^+$
M*5	7.52–7.61	264.1959	$C_{16}H_{25}NO_2^+$	0.34	246.1847	$C_{16}H_{23}NO^+$

(*continued on next page*)

Table 2 (*continued*)

Compound	Retention time (min)	[M+H$^+$] (*m/z*)	Elemental composition	Mass error (ppm)	Product ion (*m/z*)	Elemental composition
					228.1724	$C_{16}H_{21}N^+$
					186.1278	$C_{13}H_{16}N^+$
					174.1275	$C_{12}H_{14}O^+$
					118.0491	$C_8H_7O^+$
M*6-M*7	7.36–7.76	278.1750	$C_{16}H_{23}NO_3^+$	0.25	260.1634	$C_{16}H_{21}NO_2^+$
					242.1541	$C_{16}H_{19}NO^+$
					186.0914	$C_{12}H_{12}NO^+$
					174.1275	$C_{12}H_{14}O^+$
					157.0995	$C_{12}H_{13}^+$
					105.0335	$C_7H_5O^+$
M*8	11.35	260.1646	$C_{16}H_{21}NO_2^+$	0.30	242.1541	$C_{16}H_{19}NO^+$
					224.1391	$C_{16}H_{17}N^+$
					175.1118	$C_{12}H_{15}O^+$
					157.1007	$C_{12}H_{13}^+$
					129.0692	$C_{10}H_9^+$
					105.0331	$C_7H_5O^+$
M*9	11.13	276.1599	$C_{16}H_{21}NO_3^+$	0.50	205.0951	$C_{12}H_{13}O_3^+$
					177.0901	$C_{11}H_{13}O_2^+$
					105.0322	$C_7H_5O^+$

previously reported in pyrrolidinyl-containing molecules (Vickers and Polsky, 2000).

Finally, a tentative metabolite M6 with a retention time of 6.67 min, and a *m/z* value of 250.1444, suggested a dihydroxylation of 4-MePPP. Fragment ions at 119.0964 and 147.0804, suggested that dihydroxylation is not occurring in the phenone moiety.

3.2.2. TH-PVP metabolism

Figure 2 shows the tentative metabolic pathway of the TH-PVP and Fig. 3 shows the chromatograms, the exact mass of the pseudo-molecular ions and characteristic fragments of the parent compound and its tentatively proposed metabolites in early zebrafish after 24 h of exposure.

As it can be seen, TH-PVP parent compound presented a peak with a retention time of 10.30 min and a *m/z* value of the protonated species of 286.2124. The most intense fragment ions included 215.1849 (pyrrolidine ring loss), 159.1116 (phenone group), and 145.1292 (5,6,7,8-tetrahydronaphthalen-2-yl group).

Monohydroxylated metabolites (M'1-M'5) presented the most intense metabolite signals with *m/z* 302.2120 (Δm = 0.10 ppm). Hydroxylation of the 5,6,7,8-tetrahydronaphthalene moiety were tentatively proposed after observation of the fragments at 143.1137 and 175.1101 corresponding to $C_{11}H_{11}^+$and $C_{11}H_{11}O_2^+$, respectively. Phenyl moiety hydroxylation of the has been reported for 3F-α-PVP (Carlier et al., 2022) and 4F-α-PVP and α-PHP (Carlier et al., 2021) with human hepatocytes.

Additionally, monohydroxylated metabolites (M'6-M'8) with *m/z* 302.2120 (Δm = 0.50 ppm) at alkyl chain and pyrrolidine ring moieties were tentatively proposed after observation of the fragments at 159.1116 and 145.1292, also present in the molecule of TH-PVP, indicating that hydroxylation is not related to the 5,6,7,8-tetrahydronaphthalene moiety. Moreover, hydroxylation of the alkyl chain, pyrrolidine, and methylenedioxyphenyl moieties has been also proposed as metabolites of methylenedioxypyrovalerone (MDPV), a TH-PVP related compound (Negreira et al., 2015).

5,6,7,8-tetrahydronaphthalene moiety oxidation or hydroxylation and dehydrogenation (+O –2H) with *m/z* 300.1960 (Δm = 2.00 ppm) has been also identified (M'9) with a retention time of 8.94 min. It has been tentatively proposed after observation of the fragment 173.0936 corresponding to the formula $C_{11}H_9O_2^+$, which indicates that the second oxygen is attached to the 5,6,7,8-tetrahydronaphthalene moiety. A dihydroxylated metabolite signal (M'10) appearing at 10.13 min and *m/z* 318.2064 has been also identified as a TH-PVP metabolic transformation, similar to α-PHP and 4F-α-PVP (Carlier et al., 2021). The presence of only one peak and the fragments at 159.1116 and 145.1292, also present in the molecule of TH-PVP, suggested that only dihydroxylation in the pyrrolidinyl moiety was obtained.

M'11, with a retention time of 9.88 min and *m/z* 232.1695 (Δm = (2.60 ppm), could be due to the conversion/opening of the pyrrolidine ring to a primary amine. An analogue of this metabolite was reported for the metabolism of α-PVP in human liver microsomes (Tyrkkö et al., 2013) and in rat urine (Sauer et al., 2009).

3.2.3. α-PHP metabolism

According to the obtained MS/MS data and information of previously published papers, the molecular structure of the α-PHP

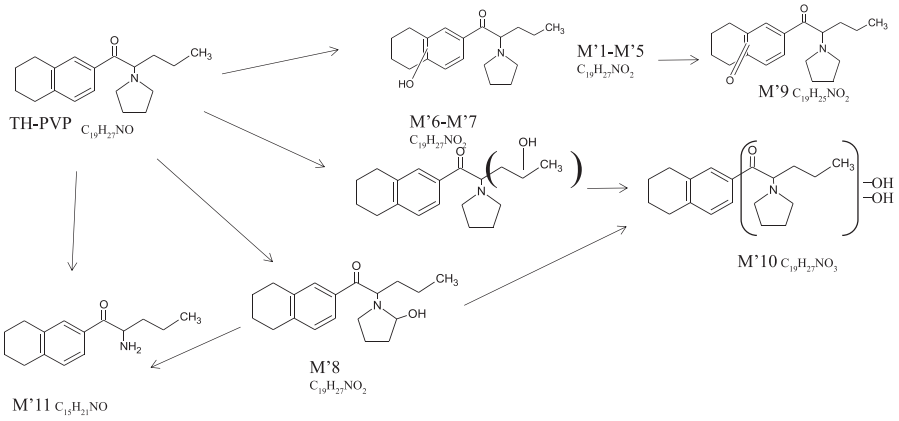

Fig. 2. Tentative metabolic pathway proposed for TH-PVP using early zebrafish larvae.

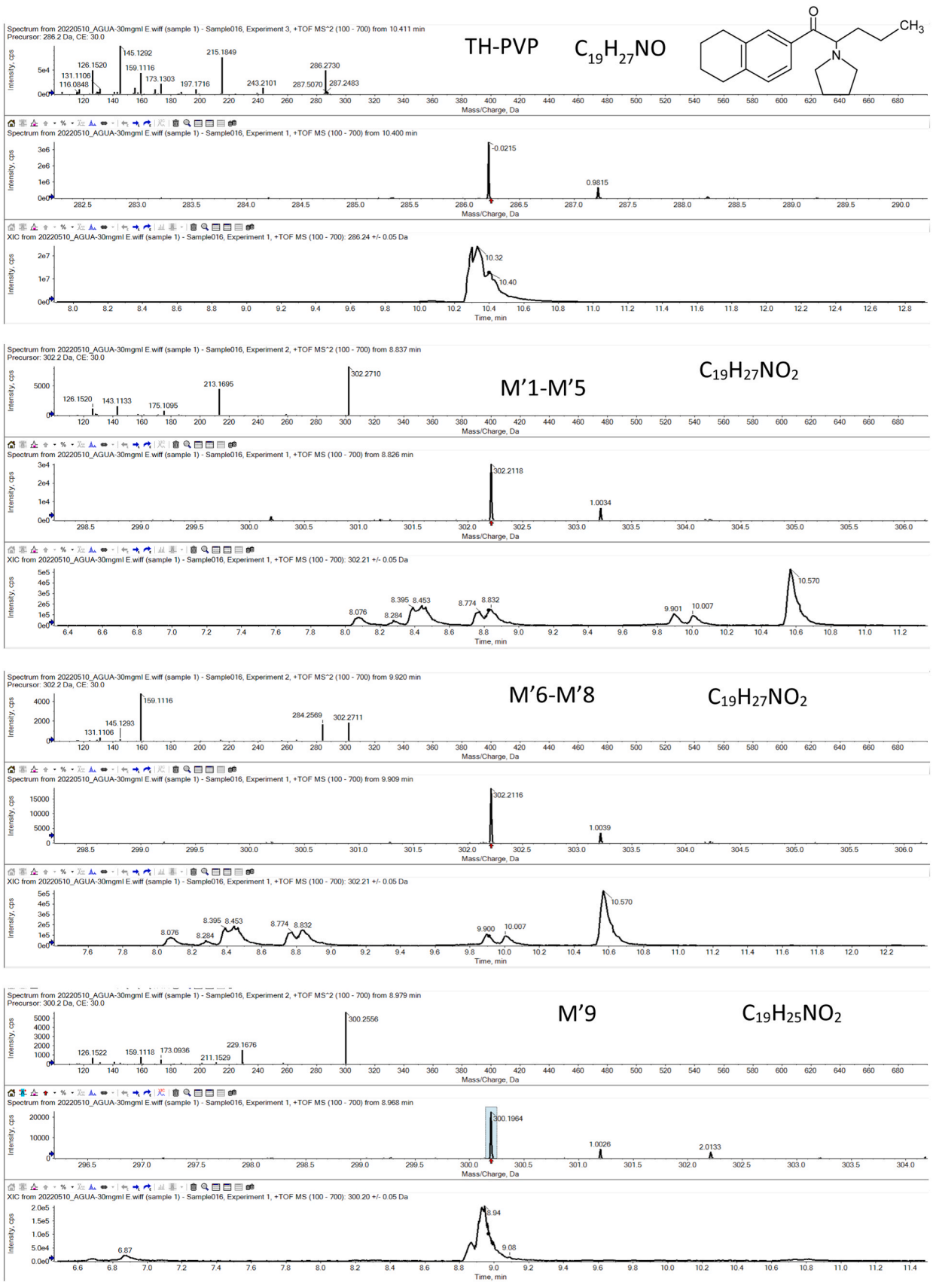

Fig. 3. Exact mass of the pseudo-molecular ions, the characteristic fragments of the parent compound, TH-PVP, and its detected metabolites and the LC-HRMS/MS chromatograms after 24 h zebrafish larvae incubation.

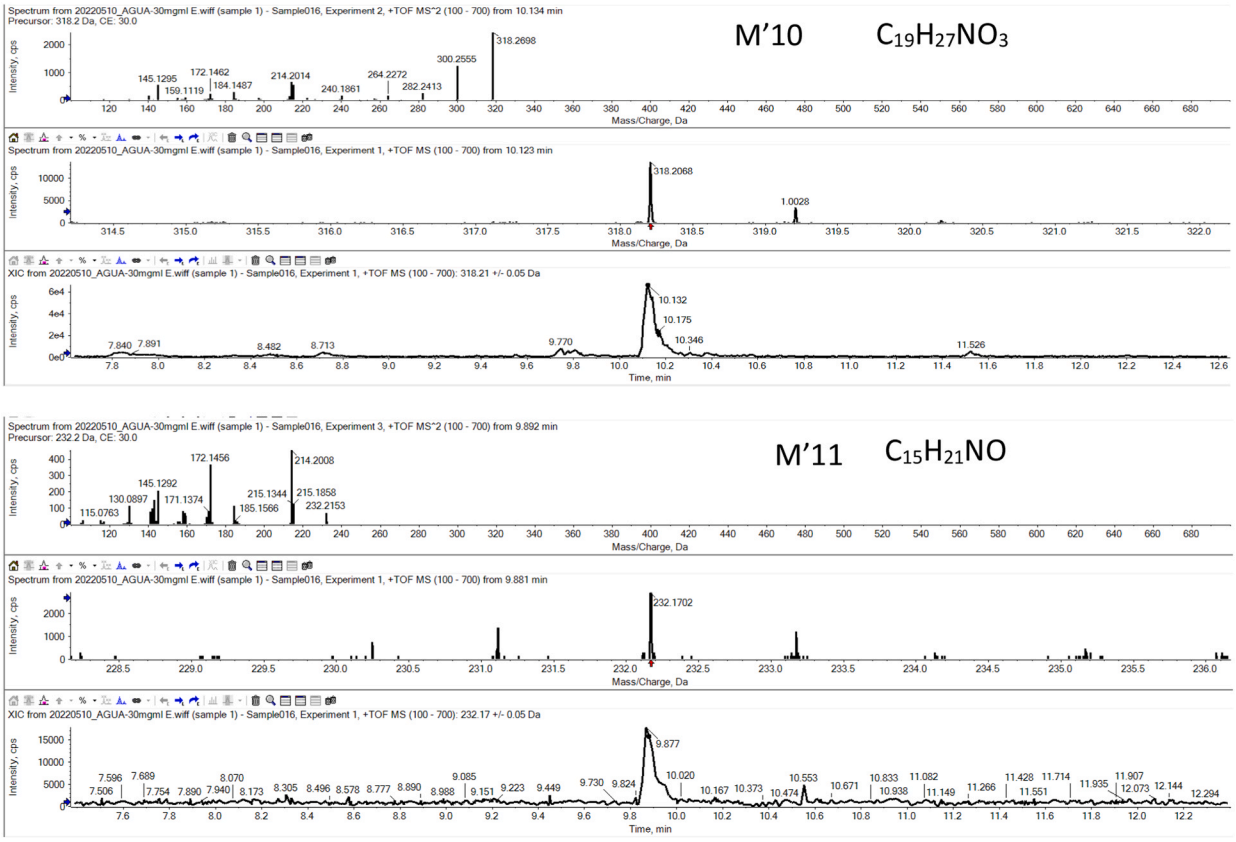

Fig. 3. (*continued*).

metabolites was tentatively proposed. Fig. SM3 shows the chromatograms, the exact mass of the pseudo-molecular ions and characteristic fragments of the parent compound and its detected metabolites.

As it can be seen, α-PHP parent compound presented a peak at 13.46 min with an *m/z* value of 246.1840. Major fragments were obtained at *m/z* 105.0332 and 140.1610, corresponding to the breakage of the molecule at the carbon adjacent to the ketone group. Other minor fragment at *m/z* 175.1117, corresponding to the loss of the pyrrolidinyl moiety was observed.

Monohydroxylated metabolite (M''1-M''2), with retention times from 13.37 to 13.48 min at *m/z* 262.1793 (Δm = 2.0 ppm), was the most intense observed signal. It is confirmed by a +15.9950 Da mass shift from the parent and the intense fragment at *m/z* 244.1693 due to a water loss. Fragment ions at *m/z* 105.0335, 140.1432 and 188.1075, indicated that the transformation occurred in the alkyl chain, but the exact position can not be determined.

Metabolite M''3 (dihydroxy- α-PHP), at a *m/z* 278.1740 and two water losses (260.1641 and 242.1532) suggested a dihydroxylation (+2O) of α-PHP. Once again, fragment ions at *m/z* 105.0334, and 174.1512 indicated that both hydroxylations occurred in the alkyl chain.

M''4 presented a retention time of (13.39–13.87) with a *m/z* value of 260.1646. The higher retention time than that of the parent compound, and the presence of fragments *m/z* 105.0464, and 175.1349, suggest that the oxidation of the pyrrolidinyl ring has occurred (Swortwood et al., 2016).

Phase II glucuronidations were not observed, in accordance with previous studies of α-PHP analogues performed in vitro and in vivo (Swortwood et al., 2016).

3.2.4. α-PHiP metabolism

Fig. SM4 shows the tentative metabolic pathway of the α-PHiP obtained from the chromatograms of the zebrafish medium and those of the larvae extracted following the recommended procedure (see Fig. SM5 and Table 2). In those chromatograms it can be observed the parent compound and metabolites formed in early zebrafish after 24 h of exposure.

α-PHiP presented a retention time of 8.10 min and an *m/z* value of 246.1852. The most intense fragment peaks were those at *m/z* 188.1137, corresponding to the dealkylation, at 140.1418, due to the loss of phenone group, at 105.0335 due to the phenone group itself, and 119.0491 corresponding to the methylphenone group.

As it can be seen in Fig. SM7, hydroxylation of the isoalkyl chain and the pyrrolidine group was observed (M*2-M*3) with an *m/z* value of 262.1810 and 262.1798, respectively. Metabolite M*2 corresponds to the mono-hydroxylation of the pyrrolidine moiety of α-PHiP, which is supported by the fragments at 157.1012 and 105.0330. On the other hand, M*3 could be assigned to the alkyl chain hydroxylation, based on the fragment at 188.1067 ($C_{12}H_{14}NO\bullet$). Other MS/MS fragments included *m/z* 244.1670, a water loss, *m/z* 156.1374, 119.0488 and 105.0323, supported the hydroxylation of alkyl chain of α-PHiP. Additionally, M*4 with an *m/z* value of 262.1784 and a retention time of 6.83 min, corresponded to a ß-keto reduction and oxidation of the pyrrodinyl moiety of α-PHiP. Fragments at *m/z* 121.0486 and 107.0485 suggests the formation of the benzyl alcohol moiety.

Metabolite M*5 with *m/z* 264.1959 ($C_{16}H_{25}NO_2$) presented a peak at 7.52–7.61 min as a result of ß-keto reduction and mono-hydroxylation at the alkyl chain of α-PHiP. Hydroxylation of the alkyl chain is supported by an intense loss of water (246.1847) and a less intense loss of a second water molecule (228.1724). Hydroxylation of the alkyl chain is also corroborated by the fragment at *m/z* 174.1275, corresponding to the loss of $C_4H_9O\bullet$. Additionally, the low abundance of *m/z* 105 is in accordance to the reduction of the ß-keto moiety. Hydroxylation of the pyrrolidine group has been reported for the α-PHiP metabolism with human hepatocytes (Kemenes et al., 2023).

Metabolite M*6–7 (*m/z* 278.1750, $C_{16}H_{23}NO_3$, mass error:

0.25 ppm) could be due to the formation of an aldehyde in the pyrrolidine ring after the oxidation and hydroxylation. It is corroborated by a high intense fragment due to the loss of water, at *m/z* 260.1634, due to a secondary alcohol, a further minor loss of water at *m/z* 242.1541. The fragments at *m/z* 174.1275 and 105.0335, corresponding to the ketone-phenyl moiety, indicated that changed occurred at the pyrrodinil group. An analogue metabolite has been previously reported for α-PVP (Negreira et al., 2015).

Other less intense metabolite peaks were obtained at *m/z* values 260.1646 (M*8) and 276.1595 (M*9), corresponding to the oxidation of the pyrrolidine moiety and carboxylation of the alkyl chain, respectively. MS/MS spectra of M*8 was characterized by two water losses (242.1541 and 224.1391), a fragment at *m/z* 175.1118 (ß-keto backbone), and an additional loss of water from $C_{12}H_{15}O^+$ to provide the fragment at 157.1007. This signature was also observed in similar compounds such as 2″-oxo-α-PVP (Shima et al., 2014). Finally, M*9, the carboxylated metabolite, was characterized by fragment ions at 205.0815 (pyrrolidine ring loss) and 177.0901 (additional CO loss).

3.3. Correlation of LC_{50} values from zebrafish larvae with mammalian species

Previous studies have demonstrated a direct correlation between LC_{50} obtained from early stages zebrafish, scored at 96 hpf, and rat, mouse, and rabbit species LC_{50} inhalation values (slope value: 0.74) (Ducharme et al., 2015). In other study, zebrafish embryo log LC_{50} values were compared with rodent log LD_{50} obtained from the literature (Ali et al., 2011). Thus, using the correlations proposed in those articles, and considering the LC_{50} obtained in our study, it could be estimated the LC_{50} inhalation values in mammals following reference (Ducharme et al., 2015) and the rodent LD_{50} according to reference (Ali et al., 2011) (see Table 3). As it can be seen in Table 3, LC_{50} inhalation values in mammals and the rodent LD_{50} ranged from 3.51 to 57.09 mg kg^{-1}. From the evaluated synthetic cathinones, TH-PVP proved to be the most toxic, whereas 4-MePPP was the less toxic. It is in accordance with previously published data, where it is stated that the presence of a longer α-alkyl side chains is related to enhanced potency to inhibit DAT (IC_{50} 0.06 μM for α-PHP versus 0.75 μM for 4-MePPP) (Kolaczynska et al., 2021). There is no published LC_{50} or LD_{50} values for the studied compounds. However, the obtained values have been compared with those of similar compounds. For instance, the LD_{50} of α-PVP administered to mice is 38.5 mg kg^{-1} (EMCDDA, 2016). LD_{50} for mephedrone is 119–143 mg kg^{-1} in mice (Serefko et al., 2022). LD_{50} values for methamphetamine and 3,4-methylenedioxymethamphetamine (MDMA) were 84.5 and 100.9 mg kg^{-1} in mice (Muskiewicz et al., 2020). In this study, the LD_{50} value obtained for methyl-methcathinone was 118.8 mg kg^{-1} and related compounds, such as cathinone, methcathinone and 3,4-methylenedioxypyrovalerone (MDPV) presented limited lethality, so LD_{50} values could not be calculated. Other study, reported a LD_{50} value of 43.2 mg kg^{-1} for methamphetamine in mice (Ginawi et al., 1997). The LD_{50} of amphetamine was 23.3 mg kg^{-1} administered orally and 5.9 mg kg^{-1} intravenously (Zalis et al., 1964).

Finally, LD_{50} values of other drugs have been reported, including heroin (21.8 mg kg^{-1} in mice and 22.5 mg kg^{-1} in rat, cocaine (16 mg kg^{-1} in mice and 17.5 mg kg^{-1} in rat), Δ^9-tetrahydrocannabinol (THC) (482–666 mg kg^{-1} in rat), nicotine (3.34 mg kg^{-1} in mice and 50 mg kg^{-1} in rat) and amphetamine (21 mg kg^{-1} in mice and 30 mg kg^{-1} in rat) (Lachenmeier and Rehm, 2015).

4. Conclusions

For the first time, LC_{50} of α-PHP, α-PHPiP, 4-MePPP and TH-PVP, has been obtained using zebrafish larvae. All the tested substances exhibited an increase of the acute toxicity with exposure time and, as it can be derived from the acute toxicity experiments, the embryo chorion did not act as a barrier for this kind of abuse substances. From the evaluated synthetic cathinones, TH-PVP proved to be the most toxic, whereas 4-MePPP was the least toxic. Moreover, from the obtained LC_{50} in zebrafish embryos scored at 96 hpf, LC_{50} values of other rodent species can be estimated using previous correlation studies. On the other hand, the metabolism of these compounds has been studied using early zebrafish larvae. The results showed that hydroxylation and dihydroxylation can be considered the main metabolic pathways, although depending of the cathinone studied, other metabolites can be found.

In summary, the obtained results have demonstrated that the zebrafish embryo toxicity test can be considered as a powerful, simple and effective tool for assessing the acute toxicity of these psychoactive substances as well as to evaluate the metabolism of this type of substances, selecting the most appropriate analytical target to evaluate human abuse.

Table 3
LC_{50} inhalation values in mammals estimated from the LC_{50} obtained from zebrafish embryos at 96 hpf.

Compound	LC_{50} Zebrafish embryos (mg L^{-1})	LC_{50} rat (mg kg^{-1})[a]	LD_{50} rodent (mg kg^{-1})[b]
α-PHP	22.30	19.40	16.37
α-PHiP	39.39	34.27	28.91
4-MePPP	65.62	57.09	48.17
TH-PVP	4.78	4.16	3.51

[a] Estimated values obtained from the regression lines of the manuscript of Ducharme et al. (2015).
[b] Estimated values obtained from the regression lines of the manuscript of Selderslaghs et al. (2009).

CRediT authorship contribution statement

M.D. Ferrando: Writing – review & editing, Supervision, Conceptualization. **S. Armenta:** Writing – review & editing, Validation, Supervision, Investigation, Funding acquisition, Conceptualization. **P. García Atienza:** Writing – original draft, Investigation, Formal analysis. **E. Sancho:** Writing – review & editing, Validation, Supervision, Investigation, Formal analysis, Conceptualization.

Declaration of Competing Interest

The authors declare that they have no known competing financial interests or personal relationships that could have appeared to influence the work reported in this paper.

Acknowledgements

Authors gratefully acknowledge the financial support of the project PID2019-110788GB-I00 funded by Ministerio de Ciencia, Innovación y Universidades, Spain (MCIN/AEI/10.13039/501100011033) and the technical support from M. Sales Galletero from the SCSIE of the University of Valencia.

Appendix A. Supporting information

Supplementary data associated with this article can be found in the online version at doi:10.1016/j.ecoenv.2024.117174.

Data availability

Data will be made available on request.

References

Adamowicz, P., Jurczyk, A., Gil, D., Szustowski, S., 2020. A case of intoxication with a new cathinone derivative α-PiHP – a presentation of concentrations in biological specimens. Leg. Med. https://doi.org/10.1016/j.legalmed.2019.101626.

Ali, S., van Mil, H.G.J., Richardson, M.K., 2011. Large-scale assessment of the zebrafish embryo as a possible predictive model in toxicity testing. PLoS ONE. https://doi.org/10.1371/journal.pone.0021076.

Carlier, J., Berardinelli, D., Montanari, E., Sirignano, A., Di Trana, A., Busardò, F.P., 2022. 3F-α-pyrrolydinovalerophenone (3F-α-PVP) in vitro human metabolism: multiple in silico predictions to assist in LC-HRMS/MS analysis and targeted/untargeted data mining. J. Chromatogr. B Biomed. Appl. https://doi.org/10.1016/j.jchromb.2022.123162.

Carlier, J., Diao, X., Giorgetti, R., Busardò, F.P., Huestis, M.A., 2021. Pyrrolidinyl synthetic cathinones α-php and 4f-α-pvp metabolite profiling using human hepatocyte incubations. Int. J. Mol. Sci. https://doi.org/10.3390/ijms22010230.

Cassar, S., Adatto, I., Freeman, J.L., Gamse, J.T., Iturria, I., Lawrence, C., Muriana, A., Peterson, R.T., Van Cruchten, S., Zon, L.I., 2020. Use of zebrafish in drug discovery toxicology. Chem. Res. Toxicol. *33* (1), 95–118. https://doi.org/10.1021/acs.chemrestox.9b00335.

Castiglioni, S., Salgueiro-González, N., Bijlsma, L., Celma, A., Gracia-Lor, E., Beldean-Galea, M.S., Mackuľak, T., Emke, E., Heath, E., Kasprzyk-Hordern, B., Petkovic, A., Poretti, F., Rangelov, J., Santos, M.M., Sremački, M., Styszko, K., Hernández, F., Zuccato, E., 2021. New psychoactive substances in several European populations assessed by wastewater-based epidemiology. Water Res. *195*, 116983. https://doi.org/10.1016/j.watres.2021.116983.

Chen, Y., Canal, C.E., 2020. Structure–activity relationship study of psychostimulant synthetic cathinones reveals nanomolar antagonist potency of α-pyrrolidinohexiophenone at human muscarinic M_2 receptors. ACS Chem. Neurosci. *11* (6), 960–968. https://doi.org/10.1021/acschemneuro.0c00008.

Colwill, R.M., Creton, R., 2011. Imaging escape and avoidance behavior in zebrafish larvae. Revneuro *22* (1), 63–73. https://doi.org/10.1515/rns.2011.008.

Contrucci, R.R., Brunt, T.M., Inan, F., Franssen, E.J.F., Hondebrink, L., 2020. Synthetic cathinones and their potential interactions with prescription drugs. Ther. Drug Monit. *42* (1), 75–82. https://doi.org/10.1097/FTD.0000000000000682.

Coppola, M., Mondola, R., 2012. Synthetic cathinones: chemistry, pharmacology and toxicology of a new class of designer drugs of abuse marketed as " bath salts" or " plant food.". Toxicol. Lett. https://doi.org/10.1016/j.toxlet.2012.03.009.

De Felice, B., Mondellini, S., Salgueiro-González, N., Castiglioni, S., Parolini, M., 2020. Methamphetamine exposure modulated oxidative status and altered the reproductive output in *Daphnia magna*. Sci. Total Environ. *721*, 137728. https://doi.org/10.1016/j.scitotenv.2020.137728.

De Oliveira Eiras, M.I., Costa, L.S. da, Barbieri, E., 2022. Copper II oxide nanoparticles (CuONPs) alter metabolic markers and swimming activity in zebra-fish (*Danio rerio*). Comp. Biochem. Physiol. C Toxicol. Pharmacol. *257*, 109343. https://doi.org/10.1016/j.cbpc.2022.109343.

Drug Enforcement Administration & Department of Justice, 2016. "Schedules of Controlled Substances: Placement of 10 Synthetic Cathinones Into Schedule I." 81: 11479-11486. Document Number: 2016-05002. Document Citation: 81 FR 11479. ⟨https://www.federalregister.gov/documents/2016/03/04/2016-05002/schedules-of-controlled-substances-placement-of-10-synthetic-cathinones-into-schedule-i⟩ (Last accessed 14-09-2023).

Drug Enforcement Administration and Department of Justice, 2018. "Schedules of Controlled Substances: Temporary Placement of N-Ethylpentylone in Schedule I." 83: 27520-27520. Document Number: 2018-12669. Document Citation: 83 FR 27520. ⟨https://www.federalregister.gov/documents/2018/06/13/2018-12669/schedules-of-controlled-substances-temporary-placement-of-n-ethylpentylone-in-schedule-i⟩ (Last accessed 14-09-2023).

Ducharme, N.A., Reif, D.M., Gustafsson, J.A., Bondesson, M., 2015. Comparison of toxicity values across zebrafish early life stages and mammalian studies: Implications for chemical testing. Reprod. Toxicol. https://doi.org/10.1016/j.reprotox.2014.09.005.

EMCDDA, 2016. Report on the Risk Assessment of 1-phenyl-2-(pyrrolidin-1-yl)pentan-1-one(α-pyrrolidinovalerophenone, α-PVP) in the Framework of the Council Decision on New Psychoactive Substances.

EMCDDA, 2024. European Drug Report 2024: Trends and Developments.

Eshleman, A.J., Wolfrum, K.M., Reed, J.F., Kim, S.O., Swanson, T., Johnson, R.A., Janowsky, A., 2017. Structure-activity relationships of substituted cathinones, with transporter binding, uptake, and release. J. Pharmacol. Exp. Ther. *360*, 33–47. https://doi.org/10.1124/jpet.116.236349.

European Parliament & The Council Of The European Union, 2010. Directive 2010/63/EU of the European Parliament and of the Council of 22 September 2010 on the protection of animals used for scientific purposes. Off. J. Eur. Union. ⟨https://eur-lex.europa.eu/legal-content/EN/TXT/?uri=CELEX%3A02010L0063-20190626⟩.

Garcia, G.R., Noyes, P.D., Tanguay, R.L., 2016. Advancements in zebrafish applications for 21st century toxicology. Pharmacol. Ther. *161*, 11–21. https://doi.org/10.1016/j.pharmthera.2016.03.009.

Ginawi, T., Al-Shabanah, A., I Bakheet, S.A., 1997. Increased toxicity of methamphetamine in morphine-dependent mice. Gen. Pharmacol. *28*.

Goldstone, J.V., McArthur, A.G., Kubota, A., Zanette, J., Parente, T., Jönsson, M.E., Nelson, D.R., Stegeman, J.J., 2010. Identification and developmental expression of the full complement of Cytochrome P450 genes in Zebrafish. BMC Genom. *11* (1), 643. https://doi.org/10.1186/1471-2164-11-643.

González-Mariño, I., Gracia-Lor, E., Rousis, N.I., Castrignanò, E., Thomas, K.V., Quintana, J.B., Kasprzyk-Hordern, B., Zuccato, E., Castiglioni, S., 2016. Wastewater-based epidemiology to monitor synthetic cathinones use in different European countries. Environ. Sci. Technol. *50* (18), 10089–10096. https://doi.org/10.1021/acs.est.6b02644.

Kemenes, K., Hidvégi, E., Szabó, L., Szabó, S., Kerner A, Süvegh, G., 2023. Metabolism of the synthetic cathinone alpha-pyrrolidinoisohexanophenone in humans using UHPLC-MS-QToF. J. Anal. Toxicol. https://doi.org/10.1093/jat/bkac085/6774981.

Kimmel, C.B., Ballard, W.W., Kimmel, S.R., Ullmann, B., Schilling, T.F., 1995. Stages of embryonic development of the zebrafish. Dev. Dyn. https://doi.org/10.1002/aja.1002030302.

Kolaczynska, K.E., Thomann, J., Hoener, M.C., Liechti, M.E., 2021. The pharmacological profile of second generation pyrovalerone cathinones and related cathinone derivative. Int. J. Mol. Sci. https://doi.org/10.3390/ijms22158277.

Kolanos, R., Solis, E., Sakloth, F., De Felice, L.J., Glennon, R.A., 2013. "Deconstruction" of the abused synthetic cathinone methylenedioxypyrovalerone (MDPV) and an examination of effects at the human dopamine transporter. ACS Chem. Neurosci. https://doi.org/10.1021/cn4001236.

Kolesnikova, T.O., Khatsko, S.L., Eltsov, O.S., Shevyrin, V.A., Kalueff, A.V., 2019. When fish take a bath: Psychopharmacological characterization of the effects of a synthetic cathinone bath salt 'flakka' on adult zebrafish. Neurotoxicol. Teratol. https://doi.org/10.1016/j.ntt.2019.02.001.

La Maida, N., Di Trana, A., Giorgetti, R., Tagliabracci, A., Busardò, F.P., Huestis, M.A., 2021. A review of synthetic cathinone–related fatalities from 2017 to 2020. Ther. Drug Monit. *43*, 52–68.

Lachenmeier, D.W., Rehm, J., 2015. Comparative risk assessment of alcohol, tobacco, cannabis and other illicit drugs using the margin of exposure approach. Sci. Rep. https://doi.org/10.1038/srep08126.

Macrae, C.A., Fishman, M.C., 2002. Zebrafish: the complete cardiovascular compendium. Cold Spring Harb. Symp. Quant. Biol. *67* (0), 301–308. https://doi.org/10.1101/sqb.2002.67.301.

Manier, S.K., Richter, L.H.J., Schäper, J., Maurer, H.H., Meyer, M.R., 2018. Different in vitro and in vivo tools for elucidating the human metabolism of alpha-cathinone-derived drugs of abuse. Drug Test. Anal. *10* (7), 1119–1130. https://doi.org/10.1002/dta.2355.

Matos, R.R., Martucci, M.E.P., de Anselmo, C.S., Alquino Neto, F.R., Pereira, H.M.G., Sardela, V.F., 2020. Pharmacokinetic study of xylazine in a zebrafish water tank, a human-like surrogate, by liquid chromatography Q-Orbitrap mass spectrometry. Forensic Toxicol. https://doi.org/10.1007/s11419-019-00493-y.

Meyer, M.R., Du, P., Schuster, F., Maurer, H.H., 2010. Studies on the metabolism of the α-pyrrolidinophenone designer drug methylenedioxy-pyrovalerone (MDPV) in rat and human urine and human liver microsomes using GC–MS and LC–high-resolution MS and its detectability in urine by GC–MS. J. Mass Spectrom. *45* (12), 1426–1442. https://doi.org/10.1002/jms.1859.

Morales-Noé, A., Esteve-Turrillas, F.A., Armenta, S., 2022. Metabolism of third generation synthetic cannabinoids using zebrafish larvae. Drug Test. Anal. https://doi.org/10.1002/dta.3195.

Muskiewicz, D.E., Resendiz-Gutierrez, F., Issa, O., Hall, F.S., 2020. Synthetic psychoactive cathinones: hypothermia and reduced lethality compared to methamphetamine and methylenedioxymethamphetamine. Pharmacol. Biochem. Behav. https://doi.org/10.1016/j.pbb.2020.172871.

National Forensic Laboratory, 2016. Analytical report: alpha-PiHP. J. Chem. Inf. Model. https://doi.org/10.1021/ci100384d.

Negreira, N., Erratico, C., Kosjek, T., van Nuijs, A.L.N., Heath, E., Neels, H., Covaci, A., 2015. In vitro Phase I and Phase II metabolism of α-pyrrolidinovalerophenone (α-PVP), methylenedioxypyrovalerone (MDPV) and methedrone by human liver microsomes and human liver cytosol. Anal. Bioanal. Chem. https://doi.org/10.1007/s00216-015-8763-6.

OECD, 2013. "Test No. 236: Fish Ebryo Acute Toxicity (FET) Test, OECD." Guidelines for the Testing of Chemicals 2. ⟨https://doi.org/10.1787/9789264203709-en⟩.

Prado, E., Matos, R.R., de Lima Gomes, G.M., de Sá, C.B.L., da Costa Nunes, I.K., de Souza Anselmo, C., et al., 2021. Metabolism of synthetic cathinones through the zebrafish water tank model: a promising tool for forensic toxicology laboratories. Forensic Toxicol. https://doi.org/10.1007/s11419-020-00543-w.

Rickli, A., Hoener, M.C., Liechti, M.E., 2015. Monoamine transporter and receptor interaction profiles of novel psychoactive substances: para-halogenated amphetamines and pyrovalerone cathinones. Eur. Neuropsychopharmacol. https://doi.org/10.1016/j.euroneuro.2014.12.012.

Saad, M., Cavanaugh, K., Verbueken, E., Pype, C., Casteleyn, C., Van Ginneken, C., Van Cruchten, S., 2016. Xenobiotic metabolism in the zebrafish: a review of the spatiotemporal distribution, modulation and activity of Cytochrome P450 families 1 to 3. J. Toxicol. Sci. *41* (1), 1–11. https://doi.org/10.2131/jts.41.1.

Sauer, C., Peters, F.T., Haas, C., Meyer, M.R., Fritschi, G., Maurera, H.H., 2009. New designer drug α-pyrrolidinovalerophenone (PVP): studies on itsmetabolism and toxicological detection in rat urine using gas chromatographic/mass spectrometric techniques. J. Mass Spectrom. https://doi.org/10.1002/jms.1571.

Selderslaghs, I.W.T., Van Rompay, A.R., De Coen, W., Witters, H.E., 2009. Development of a screening assay to identify teratogenic and embryotoxic chemicals using the zebrafish embryo. Reprod. Toxicol. 28 (3), 308–320. https://doi.org/10.1016/j.reprotox.2009.05.004.

Serefko, A., Bielecka-Papierz, G., Talarek, S., Szopa, A., Skałecki, P., Szewczyk, B., Radziwoń-Zaleska, M., Poleszak, E., 2022. Central effects of the designer drug mephedrone in mice—basic studies. Brain Sci. https://doi.org/10.3390/brainsci12020189.

Shima, N., Katagi, M., Kamata, H., Matsuta, S., et al., 2014. Metabolism of the newly encountered designer drug α- pyrrolidinovalerophenone in humans: identification and quantitation of urinary metabolites. Forensic Toxicol. ⟨https://doi.org/10.1007/s11419-013-0202-9⟩.

Soares, J., Costa, V.M., Bastos, M., Carvalho, F., Capela, J.P., 2021. An updated review on synthetic cathinones. Arch. Toxicol. ⟨https://doi.org/10.1007/s00204-021-03083-3⟩.

Soares, J., Costa, V.M., Gaspar, H., Santos, S., de Lourdes Bastos, M., Carvalho, F., Capela, J.P., 2019. Structure-cytotoxicity relationship profile of 13 synthetic cathinones in differentiated human SH-SY5Y neuronal cells. NeuroToxicology *75*, 158–173. ⟨https://doi.org/10.1016/j.neuro.2019.08.009⟩.

Souders, C.L., Davis, R.H., Qing, H., Liang, X., Febo, M., Martyniuk, C.J., 2019. The psychoactive cathinone derivative pyrovalerone alters locomotor activity and decreases dopamine receptor expression in zebrafish (*Danio rerio*). Brain Behav. *9* (11). ⟨https://doi.org/10.1002/brb3.1420⟩.

Streisinger, G., Walker, C., Dower, N., Knauber, D., Singer, F., 1981. Production of clones of homozygous diploid zebra fish (*BrachyDanio rerio*). Nature *291*, 293–296.

Summerfield, S.G., Dong, K.C., 2013. In vitro, in vivo and in silico models of drug distribution into the brain. J. Pharmacokinet. Pharmacodyn. *40* (3), 301–314. https://doi.org/10.1007/s10928-013-9303-7.

Swortwood, M.J., Carlier, J., Ellefsen, K.N., Wohlfarth, A., Diao, X., Concheiro-Guisan, M., Kronstrand, R., Huestis, M.A., 2016. In vitro, in vivo and in silico metabolic profiling of α-pyrrolidinopentiothiophenone, a novel thiophene stimulant. Bioanalysis. https://doi.org/10.4155/bio.15.237.

Teixidó, E., Riera-Colomer, C., Raldúa, D., Pubill, D., Escubedo, E., Barenys, M., López-Arnau, R., 2023. First-generation synthetic cathinones produce arrhythmia in zebrafish eleutheroembryos: a new approach methodology for new psychoactive substances cardiotoxicity evaluation. Int. J. Mol. Sci. *24* (18), 13869. https://doi.org/10.3390/ijms241813869.

Tscharke, B.J., Chen, C., Gerber, J.P., White, J.M., 2016. Temporal trends in drug use in Adelaide, South Australia by wastewater analysis. Sci. Total Environ. *565*, 384–391. https://doi.org/10.1016/j.scitotenv.2016.04.183.

Tyrkkö, E., Pelander, A., Ketola, R.A., Ojanperä, I., 2013. In silico and in vitro metabolism studies support identification of designer drugs in human urine by liquid chromatography/quadrupole-time-of-flight mass spectrometry. Anal. Bioanal. Chem. https://doi.org/10.1007/s00216-013-7137-1.

Uchiyama, N., Shimokawa, Y., Kawamura, M., Kikura-Hanajiri, R., Hakamatsuka, T., 2014. Chemical analysis of a benzofuran derivative, 2-(2-ethylaminopropyl) benzofuran (2-EAPB), eight synthetic cannabinoids, five cathinone derivatives, and five other designer drugs newly detected in illegal products. Forensic Toxicol. https://doi.org/10.1007/s11419-014-0238-5.

Vickers, S., Polsky, S., 2000. The biotransformation of nitrogen containing xenobiotics to lactams. Curr. Drug Metab. https://doi.org/10.2174/1389200003338929.

Vignali, C., Moretti, M., Groppi, A., Osculati, A.M.M., Tajana, L., Morini, L., 2019. Distribution of the synthetic cathinone α-pyrrolidinohexiophenone in biological specimens. J. Anal. Toxicol. *43* (1), e1–e6. https://doi.org/10.1093/jat/bky047.

Wagmann, L., Frankenfeld, F., Park, Y.M., Herrmann, J., Fischmann, S., Westphal, F., Müller, R., Flockerzi, V., Meyer, M.R., 2020. How to study the metabolism of new psychoactive substances for the purpose of toxicological screenings—a follow-up study comparing pooled human Liver S9, HepaRG cells, and zebrafish larvae. Front. Chem. https://doi.org/10.3389/fchem.2020.00539.

Weichert, F.G., Floeter, C., Meza Artmann, A.S., Kammann, U., 2017. Assessing the ecotoxicity of potentially neurotoxic substances – evaluation of a behavioural parameter in the embryogenesis of *Danio rerio*. Chemosphere. https://doi.org/10.1016/j.chemosphere.2017.07.136.

Yao, B., Yan, S., Lian, L., Liu, D., Cui, J., Song, W., 2021. Occurrence, distribution, and potential health risks of psychoactive substances in Chinese surface waters. J. Hazard. Mater. *407*, 124851. https://doi.org/10.1016/j.jhazmat.2020.124851.

Zalis, E.G., Kaplan, G., Lundberg, G.D., Knutson, R.A., 1964. Acute lethality of the amphetamines in dogs and its antagonism by curare. Jaffe I.A. J. Lab. Clin. Med *67*, 118.